Article:
Tattersall, R (2013) The Hum: log-normal distribution and planetary–solar resonance. Pattern Recognition in Physics, 1 (1). 185 - 198. ISSN 2195-9250

https://doi.org/10.5194/prp-1-185-2013

Pattern Recogn. Phys., 1, 185–198, 2013
www.pattern-recogn-phys.net/1/185/2013/
doi:10.5194/prp-1-185-2013

Pattern Recognition in Physics
Open Access

The Hum: log-normal distribution and planetary–solar resonance

R. Tattersall

University of Leeds, Leeds, UK

Correspondence to: R. Tattersall (rog@tallbloke.net)

Received: 30 September 2013 – Revised: 11 November 2013 – Accepted: 12 November 2013 – Published: 16 December 2013

Abstract. Observations of solar and planetary orbits, rotations, and diameters show that these attributes are related by simple ratios. The forces of gravity and magnetism and the principles of energy conservation, entropy, power laws, and the log-normal distribution which are evident are discussed in relation to planetary distribution with respect to time in the solar system. This discussion is informed by consideration of the periodicities of interactions, as well as the regularity and periodicity of fluctuations in proxy records which indicate solar variation. It is demonstrated that a simple model based on planetary interaction frequencies can well replicate the timing and general shape of solar variation over the period of the sunspot record. Finally, an explanation is offered for the high degree of stable organisation and correlation with cyclic solar variability observed in the solar system. The interaction of the forces of gravity and magnetism along with the thermodynamic principles acting on planets may be analogous to those generating the internal dynamics of the Sun. This possibility could help account for the existence of strong correlations between orbital dynamics and solar variation for which a sufficiently powerful physical mechanism has yet to be fully demonstrated.

1 Introduction

An epoch at which a strong 2 : 1 orbital resonance existed between Jupiter and Saturn is thought to have later ejected most of the planetesimals from the system (Levison et al., 2008) and brought about the re-organisation of the planets with the planetesimal Kuiper Belt beyond Neptune. These are now found in log-normally distributed stable orbits which are close to but not at destructively resonant frequencies. The stability of the solar system at the present epoch is, however, not due to the avoidance of resonance through randomness.

As can be seen in Lykawka and Mukai (2007, Fig. 3) the semi-major axes of planetesimals in the Kuiper Belt cluster at equivalent orbital periods resonant with Neptune in the ratios 2 : 1, 3 : 2, 4 : 3, 5 : 2, 5 : 3, 5 : 8, 7 : 4, and 9 : 4. The 3 : 2 resonance is the strongest of these. It is apparent in many other solar system ratio pairs including the differential rotation of the Sun, spin–orbit ratios of Mercury and Venus, and the rates of precession of synodic conjunction cycles.

As the following observations demonstrate, these evident patterns strongly suggest that the stability of the solar system is maintained by the interaction of the gravity and the heliomagnetic field acting on planets to bring about a variety of resonant couplings. The power laws of gravity and magnetism also evidently act to bring about a log-normal distribution conforming to the numerical series which converge to phi, such as the Fibonacci and Lucas series. The timing patterns generated by the motion of the planets relative to one another are well correlated to solar variation and changes in Earth's length of day. This is further evidence suggesting that a cybernetic feedback is operating in the solar system. The effects evidently assist in maintaining stability, rather than leading to positive feedback and destructive resonance. According to Koyré (1973), Johannes Kepler, in his treatise "Nova Astonomia" wrote: "… because the Earth moves the Moon by its species, and is a magnetic body; and because the sun moves the planets in a similar manner by the species which it emits, therefore the Sun, too, is a magnetic body."

This insight may prove to be prescient, if it is eventually found that the effects of the forces of gravity and magnetism interact to bring about the simple harmonic ratios observed

Table 1. Relationships between the semi-major axes (SMA) of the solar system planets.

Planet Pair	Ratio of SMAs	Error (%)	Add/subtract unity to/from ratio units	Simplified SMA ratios
Mercury–Venus	28 : 15	0.07	28 : (15 – 1) = 28 : 14	2 : 1
Venus–Earth	18 : 13	0.15	18 : (13 – 1) = 18 : 12	3 : 2
Earth–Mars	32 : 21	0.01	(32 + 1) : (21 + 1) = 33 : 22	3 : 2
Mars–Jupiter	34 : 10	0.44	(34 + 1) : 10 = 35 : 10	5 : 2
Jupiter–Saturn	11 : 6	0.002	(11 + 1) : 6 = 12 : 6	2 : 1
Saturn–Uranus	344 : 171	0.004	344 : (171 + 1) = 344 : 172	2 : 1
Uranus–Neptune	47 : 30	0.01	(47 + 1) : 30 = 48 : 30	8 : 5

Table 2. Proximity of solar system orbital period ratios to resonant ratios.

Planet pair	Ratio of orbital periods	Error	Add/subtract unity to/from ratio units	Simplified orbital ratios
Mercury–Venus	23 : 9		(23 + 1) : 9 = 24 : 9	8 : 3
Venus–Earth	13 : 8		(13 – 1) : 8 = 12 : 8	3 : 2
Earth–Jupiter	83 : 7		(83 + 1) : 7 = 84 : 7	12 : 1
Mars–Jupiter	19 : 3		(19 – 1) : 3 = 18 : 3	6 : 1
Jupiter–Saturn	149 : 60		(149 + 1) : 60 = 150 : 60	5 : 2
Uranus–Neptune	102 : 52		102 : (52 – 1) = 102 : 51	2 : 1

between planetary and solar orbital and rotational timings. The resonances which arise from these harmonic ratios were recognised by Kepler as "The music of the spheres", and in the modern idiom, we can refer to these inter-related solar system resonances as "The Hum".

This paper examines the relationships of ratios observed in the solar system. In Sect. 2, close-to-resonant ratios are shown between planets and their synodic periods. Section 3 extends these observations to show that as well as being close to resonant ratios as planet pairs, the entire solar system lies in close relation to the log-normally distributed Fibonacci series. Section 4 shows that as well as orbital and synodic periods, the rotation rate ratios of the planet pairs are also related to the Fibonacci series. In Sect. 5 an overview of the long-term convergences and ratios of the orbital and synodic periods is given and the observations summarised.

In Sect. 6 periodicities identified in terrestrial proxy data (^{14}C and ^{10}Be) are compared with synodic periods and the number series they form, which also relate to the Fibonacci series and powers of the irrational number phi, which this series' adjacent ratios converge to. Since these proxies relate to solar activity levels, a method of correlating the planetary interaction timings of Jupiter, Earth, and Venus with solar variation is demonstrated.

Results are discussed in Sect. 7. The possible mechanisms underlying the apparently coupled phenomena are considered in relation to analogous phenomena for which theory is already developed. This discussion leads to the paper's conclusions given in Sect. 8.

2 Periodic resonance

Traditionally, the distribution of planets in the solar system has been characterised by the spacing of their semi-major axes (Bode–Titius). A short survey of the ratios between the semi-major axes of adjacent planets reveals an unusual feature whereby their almost exact ratios can be converted to a simple ratio by the addition/subtraction of unity to/from one side of the ratio, as seen in Table 1.

It should be noted that this type of relationship is not limited to the solar system. Star HD 200964 is orbited by two gas giants with orbital periods of 830 days and 630 days (Johnson et al., 2011). These periods put their semi-major axes in the ratio 6 : 5. Subtracting unity from 5 makes the ratio 3 : 2. The ratio between their orbital periods is 63 : 83. Adding unity to 83 makes the ratio 3 : 4, a resonant ratio. Similar situations occur with the ratios of orbital periods in the solar system, summarised in Table 2.

Many of the ratios in Table 2 are not strongly resonant. However, resonances which are capable of transferring angular momentum between planets and moons are evident in the ratios between the periods of synodic cycles and the orbital periods of more massive planets such as Jupiter. To understand the numerical phenomenon observed in the ratios of planets' semi-major axes seen in Table 1, we need to investigate not only the relationships between the planets' orbital periods seen in Table 2 but also their synodic cycles, which also help determine those semi-major axes via stronger resonances appearing periodically as gravitational perturbations. These are summarised in Table 3.

Table 3. Inner solar system relations with Jupiter.

Planet–planet pair	Period (years)	Ratio of relations	Error (%)	Add/subtract unity to/from ratio units	Simplified ratios	Deviation (%)
Me–Ve synodic cycle Ea–Ve synodic cycle	1.97 7.99	215 : 53	0.01	(215 + 1) : (53 + 1) = 216 : 54	4 : 1	1.3
Me–Ve synodic cycle Jupiter orbital period	1.97 11.86	6 : 1	0.33	6 : 1	6 : 1	0.33
Ratio of ratios above					3 : 2	1.05
Ea–Ve synodic cycle Jupiter orbital period	7.99 11.86	46 : 31	0.03	(46 – 1) : (31 – 1) = 45 : 30	3 : 2	1.05
Ea–Ma synodic Jupiter orbital period	4.27 11.86	50 : 9	0.005	50 : (9 + 1) = 50 : 10	5 : 1	10

3 Log-normal distribution of periodic phenomena

It is found that the orbital and synodic periods of all the planets and the two main dwarf planets Pluto and Eris lie close to simple relations with the log-normally distributed Fibonacci series, a simply generated sequence of ratios which rapidly converges towards the irrational number phi. A time period of sufficient length to cover the periodicities within the scope of this paper is considered in relation to the Fibonacci series.

In Table 4, the highest number in the Fibonacci series used (6765) is allowed to stand for the number of orbits of the Sun made by Mercury, the innermost planet. The number of orbits made by the other planets and dwarf planets during the time period of ~1630 yr is calculated. Additionally, the number of synodic conjunctions between adjacent planet pairs made in the same period is calculated using the method derived by Nicolaus Copernicus: Period = 1/((1/faster orbit) – (1/slower orbit))

The results are then compared to the descending values of the Fibonacci series and the deviations from the series calculated. Juno is selected as representative of the Asteroid Belt as it lies near the middle of the main core at a distance of 2.67 AU (Fig. 1). By Kepler's third law this object has an orbital period of $P = \sqrt{2.67^3} = 4.36$ yr.

The synodic conjunction cycles of principal planet pairs form distinctive geometric shapes with respect to the sidereal frame of reference. Mercury–Venus and Venus–Earth conjunctions return close to their original longitudes after 5 synodic conjunctions forming five-pointed star shapes, Jupiter and Saturn after 3 synodic conjunctions forming a triangle shape, and Uranus and Neptune after 21 synodic conjunctions which alternately occur nearly oppositely. The numbers 3, 5, and 21 are all Fibonacci numbers. The time periods over which these synodic conjunction cycles precess either completely or by subdivisions of the number of synodic conjunctions in their cycles relate to each other by simple numerical operations also involving Fibonacci numbers. Their ratios are included in Table 2 in red for further discussion in Sect. 4.1.

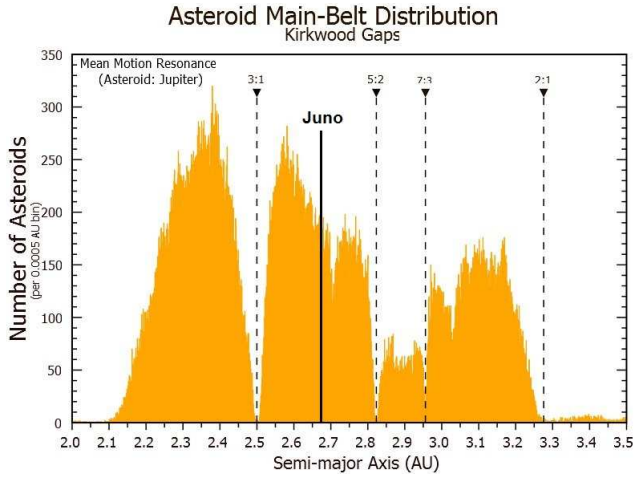

Figure 1. Dwarf planet Juno in relation to the main Asteroid Belt.

PSD analysis of the sunspot record reveals cyclic concentrations of higher sunspot numbers near the Schwabe, 1/2 Jupiter–Saturn synodic, and Jupiter orbital periods (Scafetta, 2012a). The relationship of these periods to planetary interaction periods is included, along with terrestrial climate cycle periods relating to luni–solar variation evident in proxy records such as the De Vries and Halstatt cycles.

4 Sidereal planetary rotation

4.1 The adjacent planetary pairs

It is observed in Table 5 that the numbers of completed sidereal axial rotations made by adjacent planets in proximate elapsed times form close-to-whole number ratios whose numerators and denominators sum to numbers in the Fibonacci sequence. Additional non-adjacent pair ratios are included in Table A1 of the Appendix. A test against a set of random

Table 4. Comparing the Fibonacci series to orbits and synodic conjunctions. The solar harmonics shown are the positive beat frequencies of the periods found in a power spectral density (PSD) analysis of sunspot numbers (SSN) which match the Jupiter–Saturn synodic period and the Jupiter orbital period (Scafetta, 2012b). The synodic precession cycles have simple relationships: Uranus–Neptune ~ 3600 yr is in 2 : 3 ratio with Jupiter–Saturn ~ 2400 yr, which is in 1 : 2 ratio with Earth–Venus ~ 1200 yr. One-fifth of the latter is in 1 : 5 ratio with Venus–Mercury ~ 48 yr. This suggests coupled relationships.

Fibonacci number	Period (years)	Period (years)	Relationship	Number of cycles	Deviation
6765	0.24	0.24	Orbit	6765: Mercury	+0 (baseline)
4181	0.389	0.395	Synodic	4162.2: Mercury–Venus	+0.46 %
2584	0.63	0.615	Orbit	2628.1: Venus	−1.72 %
1597	1.02	1	Orbit	1629.7: Earth	−2.04 %
987	1.65	1.6	Synodic	1019.41: Venus–Earth	−3.28 %
610	2.67	2.67	Destructive resonance orbit		
377	4.32	4.36 4.27	Orbit Synodic	372.9: Juno 381.4: 2 × Earth–Mars	+1.1 % −1.18 %
233	6.99	6.99 6.99 6.89	Harmonic Harmonic Synodic	232.955: J-S+Solar10.8yr 232.85: 2×J+0.5J-S:PSD-SSN 235.3: Juno–Jupiter	−0.01 % +0.07 % −1.1 %
144	11.32	11.28 11.86 11.07	Orbit Orbit Harmonic	144.4: 6 × Mars 137.4: Jupiter 147.7 Schwabe cycle	−0.27 % +4.6 % −2.2 %
89	18.31	19.86	Synodic	82.1: Jupiter–Saturn	+4.1 %
55	29.63	29.46 30 29.77	Orbit Harmonic Synodic	55.3: Saturn 54.32: 1/2 × AMO 54.74: 9 × Mars–Juno	−0.43 % +1.3 % +0.48 %
34	47.93	47.5 45.36	Synodic precession cycle Synodic	34.28 Mercury–Venus 35.93: Saturn–Uranus	−0.9 % −5.4 %
21	77.6	84.01	Orbit	19.4: Uranus	+7.6 %
13	125.4	122.04	Harmonic	13.36: 2 × J+J-S PSD-SSN	−2.77 %
8	203.7	247.67 208	Orbit Harmonic	7.6: Pluto 7.83: De Vries cycle	+5.26 % +2.1 %
5	325.9	329.58 342.78	Orbit Synodic	4.9: 2 × Neptune 4.75: 2 × Uranus–Neptune	+2.0 % +5.0 %
3	543.2	557 492.44	Orbit Synodic	2.9: Eris 3.31: Neptune–Pluto	+2.5 % −10.7 %
2	814.9	796	Synodic precession cycle	2.04: 1/3 Jupiter–Saturn	−2.4 %
1	1629.7	1601 1598.6 1617.7	Harmonic Synodic precession cycle Synodic precession cycle	0.98 2/3 Halstatt cycle 0.98: 4/3 Venus–Earth 0.99: 4/9 Uranus–Neptune	−1.7 % −1.9 % −0.8 %
				Average deviation of relationships from the Fibonacci series Sum of all deviations	2.51 % −2.23 %

rotation periods finds that the set of real rotation periods has 50 % lower numbers in their ratios (Appendix Table A2).

Solar rotation and the terrestrial planets: Sun and Mercury

Notwithstanding the Sun's axial tilt with respect to the invariant plane, the planets approximately orbit the Sun's equator. Due to its proximity to the Sun, Mercury has a higher orbital inclination from the plane of invariance than other planets, being more affected by the quadrupole moment from the Sun's slight equatorial bulge. The sidereal solar equatorial rotation rate is such that a fixed point on the solar equator lies directly between Mercury and the solar core every 33.899 days. From the frame of reference of solar rotation, Mercury makes exactly one axial rotation every two sidereal orbits, while Mercury completes exactly three axial rotations in the sidereal frame of reference during those two orbits. The Fibonacci numbers involved in this relationship are 1, 2, and 3.

4.2 Mercury and Venus

This planet pair forms a synodic conjunction every 144.565 Earth days, advancing 142° in the sidereal frame of reference. Every fifth conjunction is formed within 8° of the first, during a period of 1.97 yr. The precession of this sequence translates the longitude of one conjunction to the adjacent synodic conjunction point 142° away over a period of 18.72 yr. Within 9 days of this period Venus completes 28 sidereal axial rotations, while Mercury completes 116 (see Table 2) Adding unity to 28 creates a 4 : 1 ratio. The precession of the five-conjunction cycle takes on average 47.53 yr. After five of these 47.53 yr periods, plus one more five-synod cycle of 1.97 yr, the five-synod-conjunction cycle of Venus and Earth precesses 1/5 in 239.8 yr. The Fibonacci numbers involved in this relationship are 5 and 144.

Every 28 synodic conjunctions, Venus completes 18 orbits and Mercury completes 46 orbits. In this same period Mercury completes exactly 69 axial rotations. Therefore Mercury presents the same face to Venus every 28 synodic conjunctions. This is also the length of the Jupiter–Earth–Venus cycle. It is also the same period of time as the average solar cycle length (11.08 yr).

4.3 Venus and Earth

The planet Venus has a slow, retrograde axial rotation period of 243.013 days. Due to the relative rates at which Venus and Earth orbit the Sun, this means Venus will present the same face to Earth each time they meet in synodic conjunction, every 1.598 yr. This also means Venus' sidereal axial rotation is in a 3 : 2 relationship with Earth's orbital period. As seen from Earth, Venus completes two rotations in the same period.

Every 13 orbits of Venus, Earth orbits 8 times and they form 5 synodic conjunctions, the final one occurring near the sidereal longitude of the first. This conjunction cycle precesses by 1/5 in 239.8 yr after exactly 150 conjunctions. The full precession cycle is 1199 yr, and this period is close to a 3 : 2 ratio with the synodic conjunction longitude translation period of the Jupiter–Saturn synodic cycle precession of 796 yr. A closer ratio is 360 : 239. The former number of the ratio, 360, is 3 times the number of Jupiter–Saturn synodic periods in the full precession of the "triple conjunction cycle". The latter number, 239, is also the number of completed Earth orbits in 1/5 of the Earth–Venus synodic precession period of 1199 yr.

A further observation linking the rates of axial rotation and orbital motion of these three terrestrial planets and the Sun is the fact that Mercury rotates 4.14 times in the same time that Venus rotates once, and Mercury completes 4.15 orbits of the Sun while Earth orbits once.

To further underline the non-random nature of the orbital arrangement of these planets and their axial rotation periods, it is observed that the ratio of Venus and Earth's rotation rates divided by their orbital periods is 1.08 : 0.0027. This is equivalent to the ratio 400 : 1. During their respective synodic periods with Jupiter, Venus completes 1.03 rotations and Earth completes 398.88. Venus would not be able to fulfil a near 1 : 1 rotation per synod relationship with both Earth and Jupiter if it were rotating prograde. The force of gravity exerted on Venus by Jupiter and the Earth is of a similar magnitude. This suggests that a transfer of angular momentum is taking place and an orbit–spin coupling is operating to synchronise Venus' orbital and spin relations with these two planets.

The Fibonacci numbers involved in these relationships are 2, 3, 5, 8, and 13

4.4 The gas giant planets

Rotation

As we saw in Table 2, the rotation rate ratios of both the outer and inner pairs of the Jovian group is 46 : 43. The other adjacent pair in the group is Uranus–Saturn, in a 2 : 3 ratio. The ratio between the outer and inner pair's summed rotation periods is 1.618 or phi.

That calculation uses a figure of 642 min for Saturn's rotation. However, the radio signals on which the rotation rate is based are variable. Starting with the combined figures, and assigning a notional average of 642 to Saturn, Ur + Ne = 2001 min. Ju + Sa = 1237.5 min. Dividing to obtain the ratio, 2001/1237.5 = 1.617. Since phi is just over 1.618 it is an extremely close match.

Ur / Ju = 1.623. Ne / Sa = 1.611 (using 642 min for Saturn rotation) = 1.624 (using 637 min) = 1.599 (using 647 min)

Table 5. Comparing the Fibonacci series to rotation ratios. Saturn's rotation rate is variable according to the radio signal metric used as the metric. Figures in bold indicate members of the Fibonacci series.

Primary pairs	Rotation period	Rotations	Elapsed time	Ratio/sum	% match	Notes
1 Mercury 2 Venus	58.65 days 243.02 days	116 28	6803.4 d 6804.56 d	116 : 28 = **144**	99.983	
1 Earth 2 Mars	24 hours 24.6229 hours	118 115	2832 h 2831.6335 h	118 : 115 = **233**	99.987	
1 Jupiter 2 Saturn	595.5 min 640 min (N1)	46 43	27 393 min 27 520 min	46 : 43 = **89**	Up to 100 (variable)	(N1) Re. Saturn: 637.0465 = 100 % match (N1) Sat. rotation varies: est. 636–648 min
1 Uranus 2 Neptune	16.11 hours 17.24 hours	46 43	741.06 h 741.32 h	46 : 43 = **89**	99.965	
1 Pluto 2 Eris	153.29 hours 25.9 hours (N2)	8 47	1226.32 h 1217.3 h	8 : 47 = **55**	99.26	 (N2) Eris rotation may not be 100 % correct

Table 6. Comparing the Fibonacci series and synodic periods to solar proxy data from McCracken et al. (2013a). Values in bold indicate periods within the error range of the peaks found in the C^{14} and ^{10}Be spectral analysis.

Period (years)	Saturn–Uranus synodic periods	Fibonacci number	Series in proxy data	Series in proxy data	Series in proxy data
45	45.36 = 1 × 45.36 = 1× S–U	1			
90	90.72 = 2 × 45.36 = 2× S–U	2	**88** × 3/2 = **132**		
130	136.1 = 3 × 45.36 = 3× S–U	3	**130** × 8/5 = **208**		
232	226.8 = 5 × 45.36 = 5× S–U	5	**208** × 5/3 = **347**		
351	362.9 = 8 × 45.36 = 8× S–U	8	**351** × 8/5 = **562**	**282** × 8/5 = **451**	
593∗	589.7 = 13 × 45.36 = 13× S–U	13		**450** × 8/5 = **720**	
974	952.6 = 21 × 45.36 = 21× S–U	21		**705** × 8/5 = **1128**	**610** × 8/5 = **976**
1550∗	1542 = 34 × 45.36 = 34× S–U	34		**1128** × 8/5 = **1805**	**976** × 8/5 = **1562**
2403	2494 = 55 × 45.36 = 55× S–U	55			**1562** × 3/2 = **2342**

These figures range from 8/5 (1.6) to 13/8 (1.625) but on the known data all are compatible with a phi–Fibonacci relationship.

5 Orbital and synodic periods

Jupiter and Saturn's successive 19.86 yr conjunctions form a slowly precessing triangle which rotates fully in the course of 2383 yr. One additional synodic conjunction brings the elapsed time to 2403 yr. This is the longer Halstatt cycle period found in proxy records of ^{14}C and ^{10}Be. It is almost coincident with double the 1199 yr Earth–Venus synodic cycle precession period mentioned in Sect. 4.4. Fourteen Uranus–Neptune synodic conjunctions total 2399 yr. This is 2/3 of the full Uranus–Neptune precession cycle.

The close integration of the orbital, synodic, and rotation periods of the inner planets suggests that their orbital and axial rotation periods are dynamically coupled.

The pattern we observe at the larger timescale (45–2400 yr) is that the precession of the five-synodic-conjunction cycles of the terrestrial pairs is also coupled. Mercury–Venus relates by multiples of 5 to Venus–Earth, which relates to 1/3 of the precession of the triangular synodic conjunction cycle of Jupiter–Saturn in a 3 : 2 ratio. In turn, the full Jupiter–Saturn synodic precession cycle is in a 3 : 2 ratio with the Uranus–Neptune synodic precession cycle of just over 21 conjunctions totalling 3599 yr. This period is also in a 3 : 2 relationship with the longer Halstatt cycle of around 2400 yr, which is a broad, prominent peak in the ^{10}Be and ^{14}C solar proxy records. Adding the longer and shorter Halstatt periods to a total of 4627 yr, there is a convergence of 27 Uranus–Neptune and 233 Jupiter Saturn conjunctions. There are 34 × 3 Saturn–Uranus synodic conjunctions in the same period, and 4237 Jupiter–Earth synodic conjunctions, 1 % away from the Fibonacci number 4181.

The Fibonacci numbers involved in these relationships are 1, 2, 3, 5, 21, 34, 233, and 4181

Table 7. Inner solar system cyclic convergence.

Period (years)	Synodic periods	Number series	Notes
44.704	20 × Mars–Jupiter	20	= 41 – 21
44.841	21 × Mars–Earth	21	= 41 – 20
44.763	28 × Venus–Earth	28	= 69 – 21
44.774	41 × Earth–Jupiter	41	= 69 – 28 = 21 + 20
44.770	69 × Venus–Jupiter	69	= 28 + 20 + 21 = 28 + 41
44.7254	113 × Venus–Mercury	113	= 4 × 28 + 1

6 Solar-terrestrial variation and replication with planetary periods

6.1 Longer term variation

McCracken et al. (2013) identified 15 periodicities in the ^{10}Be and ^{14}C records which relate predominantly to cosmic ray modulation by solar variation. These periodicities include ~ 90, 208, 351, 517, 705, 978, and 1125 yr. McCracken et al. (2013b) will discuss possible planetary relations with these periods. Without pre-empting their work, there are some observations highly relevant to the present study which are independent from their methodology.

A number of periods evident in the data presented in McCracken et al. (2013a) are not listed but are relevant to the present study as shown in Table 6. These include periodicities at 153, 282, 450, 562, 593, 612, and 856 yr. It is observed that the multiples are within the range of the peaks and at the centre of troughs (marked "*") in the data, and follow the Fibonacci series. At 856 yr there is a triple synodic conjunction of Jupiter, Uranus, and Neptune. Table 6 shows periodicities found in McCracken et al. (2013a) against multiples of the synodic period of Saturn and Uranus. Additionally, other series of Fibonacci-ratio-linked periods found in the proxy data are shown. These require further investigation.

6.2 Medium-term solar–terrestrial variation

Prominent cycles are evident in terrestrial and solar data at the periods of the Schwabe cycle (11.07 yr), the Hale cycle (~ 22.3 yr), the Gleissberg cycle (~ 90 yr), and in terrestrial beach ridge data (~ 45, ~ 90, ~ 179 yr) (Fairbridge and Hillaire-Marcel, 1977). We have seen the Saturn–Uranus synodic period is close to the 45 yr period and its multiples. Many inner solar system synodic periods converge in the 44–45 yr range, as shown in Table 7.

This period is in 2 : 3 Hale cycle ratio with the period of the Atlantic Multi-decadal Oscillation. It is bounded on either side by the period of five Jupiter–Neptune synods (63.9 yr), and five Jupiter–Uranus synods (69.05 yr). The 44.7 yr period is also in a 1 : 2 ratio with the ~ 90 yr Gleissberg cycle and a 1 : 4 ratio with the ~ 179 yr Jose cycle (José, 1965).

Table 8. Planetary periodicities near the period of the major ocean oscillations.

Period (years)	Orbital and synodic periods	Fibonacci number
61.75	1 × 61.75 = U–N : U–S harmonic beat period	1
58.9	2 × 29.45 = 2× Saturn	2
59.58	3 × 19.86 = 3× Jupiter–Saturn	3
63.9	5 × 12.78 = 5× Jupiter–Neptune	5
66.42	5 × 11.07 = 5× Jupiter–Earth–Venus cycle	5
63.92	8 × 7.99 = 8× Venus–Earth synodic period cycle	8

Table 8 lists periods close to the ~ 60 yr period identified as an important terrestrial climate oscillation (Mörner, 2013; Scafetta, 2012b; Akasofu, 2013; Solheim, 2013). This oscillation is observed in phenomena such as the ~ 66 yr Alantic Multi-decadal Oscillation (AMO) and the ~ 60 yr Pacific Decadal Oscillation (PDO). It is in approximate 2 : 3 ratio with the 44.7 yr period and 3 : 2 ratio with the Gleissberg cycle ~ 90 yr. These interwoven relationships are suggestive of resonant effects amplifying the terrestrial responses to solar system stimuli.

At around the period of the Gleissberg cycle, the relationships in Table 9 are observed.

The resulting number series in Table 6 matches a series used in the generation of the powers of phi.

$$
\begin{aligned}
\text{Phi}^1 &= 0 + 1\ \text{Phi} = (\sqrt{5} + 1)/2 \\
\text{Phi}^2 &= 1 + 1\ \text{Phi} = (\sqrt{5} + 3)/2 \\
\text{Phi}^3 &= 1 + 2\ \text{Phi} = (2\sqrt{5} + 4)/2 \\
\text{Phi}^4 &= 2 + 3\ \text{Phi} = (3\sqrt{5} + 7)/2 \\
\text{Phi}^5 &= 3 + 5\ \text{Phi} = (5\sqrt{5} + 11)/2 \\
\text{Phi}^6 &= 5 + 8\ \text{Phi} = (8\sqrt{5} + 18)/2 \\
\text{Phi}^7 &= 8 + 13\ \text{Phi} = (13\sqrt{5} + 29)/2 \\
\text{Phi}^8 &= 13 + 21\ \text{Phi} = (21\sqrt{5} + 47)/2
\end{aligned}
$$

6.3 The Schwabe and Hale cycles

The Schwabe solar cycle averaging around 11.07 yr and the solar magnetic Hale cycle of around 22.3 yr have been extensively studied and the planetary relations investigated by several researchers, including Wilson et al. (2008) and Scafetta (2012b). The Jupiter–Earth–Venus conjunction cycle contains several periodicities including the Schwabe and Hale cycles, and the 44.7 yr inner solar system cycle. Using a modification of a model based on the planetary index devised by Hung (2007) (R. Martin, personal communication, 2010), the present author found that alignment along the Parker spiral adjusted for solar wind velocity in accordance with the reconstruction by Svalgaard and Cliver (2007) was able to replicate the general shape and varying period of the Schwabe solar cycle well, although their varying amplitudes were not well reproduced. The result is shown in Fig. 2.

Table 9. Gleissberg cycle length planetary periods.

Period (years)	Orbital and synodic periods	Number series
84.01	$1 \times 84.01 = 1\times$ Uranus orbital period	1
90.72	$2 \times 45.36 = 2\times$ Saturn–Uranus synodic period	2
88.38	$3 \times 29.46 = 3\times$ Saturn orbital period	3
88.56	$4 \times 22.14 = 4\times$ Jupiter–Earth–Venus cycle	4
89.47	$7 \times 12.78 = 7\times$ Jupiter–Neptune synodic period	7
87.89	$11 \times 7.99 = 11\times$ Venus–Earth synodic cycle	11
94.84	$29 \times 3.27 = 29\times$ Earth–Mars synodic period	29
92.59	$47 \times 1.97 = 47\times$ Venus–Mercury synodic period cycle	47

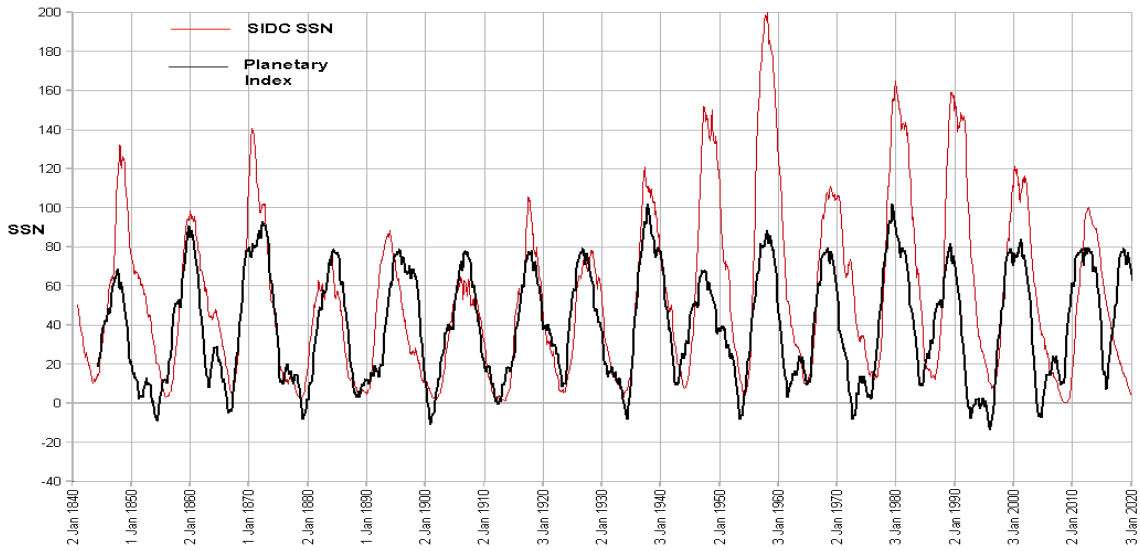

Figure 2. Reconstruction of sunspot number variation using the planetary alignment index devised by Hung (2007), modified to test alignment along the curve of the Parker spiral. Coupling this model with the solar–planetary model created by Salvador (2013) could improve the representation of amplitude and potentially lead to useful forecasting of solar variation.

7 Discussion

This paper provides observations which show that log-normally distributed numerical series which converge to phi, such as the Fibonacci and Lucas series, match the temporal–spatial distribution of matter in the solar system. Further, observations suggest that the patterns which evolve as a result of this non-random distribution of matter in the time evolution of the planetary orbits reflect changes in solar activity and the climate cycles observed on Earth. Currently, widely accepted theory concerning the evolution of the solar system considers the forces of magnetism and gravity capable of highly organising the planets' orbits and rotation rates, but the theory that the planets are capable of causing solar variation is contested (Callebaut et al., 2012, 2013; Scafetta et al., 2013).

Three theoretical mechanisms have been put forward to support the idea that the tidal and angular momentum effects of the planets could be amplified in the solar interior (Scafetta, 2012a; Wolf and Patrone, 2010; Abreu et al., 2012). The present paper adopts a different approach to tidal and angular momentum based theories by asking the following question: why phi?

As well as the convergence of the Fibonacci series to phi, the series can be generated from phi by a process of quantisation. This quantised series is log-normally distributed. The planets' orbital elements, inter-relations, and physical attributes also exhibit log-normally distributed, quantised relationships, some involving powers of phi. The following are two examples of these:

1. The inner and outer gas giant pairs' summed rotation rates are in a phi relationship, and their summed diameters are in a phi^2 relationship, to within margin of error for observation.

2. The orbital distance ratios of the Galilean moons from Jupiter can be approximated with powers of phi and more accurately calculated with Fibonacci ratios.

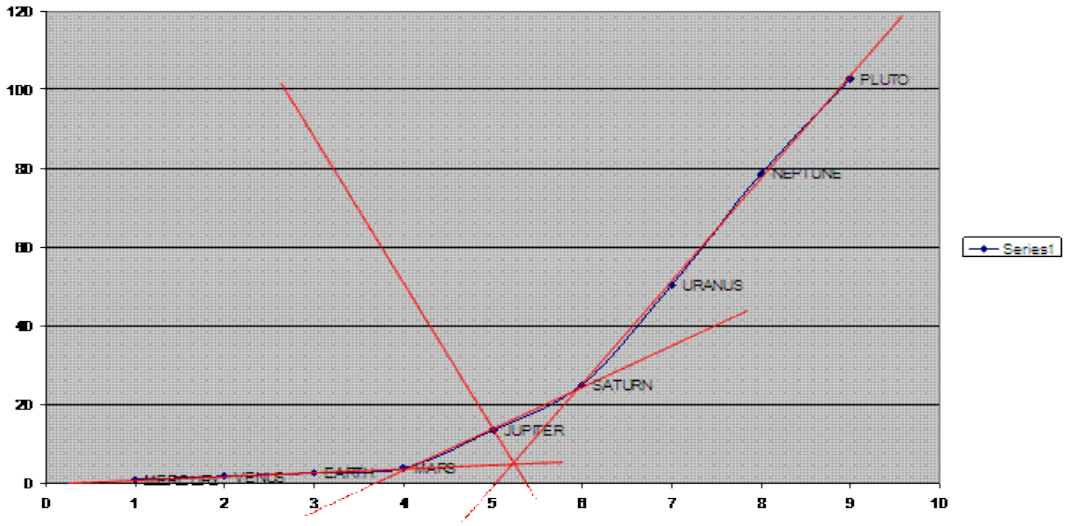

Figure 3. Planet positions against semi-major axis scaled from Earth (1) using phi^2.

The Fibonacci series has the property of containing powers of phi within itself. Adjacent numbers in the series are in approximate phi relation with their ratios converging towards phi as the series moves to higher numbers. Fibonacci numbers two positions apart in the series are in a phi^2 relationship, and those Fibonacci numbers three positions apart in a phi^3 relationship, etc.

A possible reason for the Fibonacci series evident in solar system mass and motion ratios is given by Barrow (1982):

> If we perturb a system that has a rational frequency ratio, then it can easily be shifted into a chaotic situation with irrational frequencies. The golden ratio is the most stable because it is farthest away from one of these irrational ratios. In fact, the stability of our solar system over long periods of time is contingent upon certain frequency ratios lying very close to noble numbers.

The relationship between log-normally distributed numerical series and power series has been investigated by Mitzenmacher (2004), who found that "double Pareto distributions" exhibit log-normal and power-law tails in the two halves of the distributions of randomly generated word lengths. Moreover, these power-law and log-normal distributions can interchangeably arise from randomly generated indices:

> The double Pareto distribution falls nicely between the log-normal distribution and the Pareto distribution. Like the Pareto distribution, it is a power law distribution. But while the log-log plot of the density of the Pareto distribution is a single straight line, for the double Pareto distribution the log-log plot of the density consists of two straight line segments that meet at a transition point.

Analogously, the inner and outer solar system exhibit log-normal and power-law-like tails. The difference between the Jovian outer planets and the inner solar system is illustrated in Fig. 3.

It should be noted that Jupiter's, Saturn's, and Mars' synodic periods are in 9 : 80 : 89 ratio, i.e. $9(=3\times3)$ Jupiter–Saturn $=80(=2\times5\times8)$ Jupiter–Mars $=$ 89(Fibonacci) Saturn–Mars.

It is clear that Jupiter is the transition point in the solar system: from rocky, terrestrial planets to gas giants, and from semi-major axes which scale with phi to scaling with approximate doubling. Nonetheless, all the planet pairs relate numerically with their synodic precession cycle periods in simple ratios involving Fibonacci numbers. The break point at Jupiter indicates that the outcome of force interactions and mass scales brings about a different regime in the inner and outer parts of the solar system. At the distance of the Jovian planets the Sun's gravity is weak compared to the situation in the inner solar system, and the more massive planets have a relatively much bigger effect on each other gravitationally.

What we see in the heliosphere is that which is left after 4.5 Byr evolution of the solar system. A recent model of the way in which log-normally distributed condensing gases form a star by condensation proposes that the rate of condensation is accelerated by the power law of gravity as condensation proceeds (Cho and Kim, 2011). The process causes the axial rotation to increase in rate, spinning off matter in a proto-planetary disc. Rebull (2013) proposes that the solar system's proto-planetary disc was magnetically coupled to the spinning Sun and may have acted as a brake on its rotational angular momentum. This would cause a coupling of the periodicities of solar rotation and the concentric rings of the proto-planetary disc at various distances.

Cho and Kim (2011) find that

> core (star) formation rates or core (stellar) mass functions predicted from theories based on the log-normal density PDF need some modifications. Our result of the increased volume fraction of density PDFs after turning self-gravity on is consistent with power law like tails commonly observed at higher ends of visual extinction PDFs of active star-forming clouds.

8 Conclusions

The observations made in the present study demonstrate the outcome of interactions between the power-law-based forces of gravity and magnetism and the interactions both between the Sun and planets, as well as between the planets themselves. These interactions tend to quantise their orbital and internal dynamics in ways which cause the system to evolve a log-normally distributed spatio-temporal distribution of inter-orbital relations, axial rotation rates, and orbits. The most stable interactions are in the ratios 1 : 1, 2 : 3, 3 : 5, 5 : 8, etc. This is why the Fibonacci series is the most clearly observed log-normally distributed series in the solar system. Apart from the ubiquitous 1 : 1 relationship of spin : orbit displayed by nearly every moon in the solar system tidally locked to its planet, the next most frequently observed ratio is 2 : 3. Out of the numerous examples, those most relevant to periods at which we see cycles in solar proxy records and solar observations are Mercury's 3 : 2 spin : orbit of the Sun, Venus' 3 : 2 spin against Earth's orbital period, and the 2 : 3 of Earth–Venus' synodic cycle precession period against the Jupiter–Saturn synodic cycle precession period converging at the longer Halstatt cycle length of ~ 2400 yr.

We also see 2 : 3 behaviour on the Sun itself. The rate of rotation at the equator (24.47 days) is close to a 2 : 3 ratio with the rate of rotation near the poles (~ 36 days). The rise time from Schwabe cycle minimum to maximum is, on average, in approximate 2 : 3 ratio to the period from maximum to minimum.

It is evident that the same mass distributions and forces which originally formed the Sun, a log-normally distributed gas cloud condensing under self-gravity, continue to influence its cyclic variation. The same is the case for the continual "cogging" and re-alignment of the planets as the interplay of forces with their neighbours and the Sun causes continual adjustment of their orbital periods and rates of rotation, maintaining an orderly log-normal spatio-temporal distribution.

Systems which maintain stability through cybernetic feedback oscillate about a mean. Such oscillation is observed throughout the solar system: variation in Earth's length of day, the 0.1 % variation of total solar irradiance measured during the Schwabe cycle, the long-term oscillations observed in solar proxies, and exchanges of angular momentum between Uranus and Neptune. The inexact periodic relationships undergo phase drift, and leave "standing waves" of modulated magnitude near the convergent frequencies identified in this study. To understand how the motion of the planets could be linked to terrestrial climatic variation, both via solar variation and directly, we must additionally consider the thermodynamic, gravitational, and magnetic forces to which both the planets and the Sun are currently subjected and were originally formed by.

The Sun's decadal variation in total solar irradiance is around 0.1 % of its output. If the strong correlations observed between planetary motion and solar variation are indicative of cybernetic feedback, then such a minor variation at around the orbital period of the largest planet in the system may indicate a well-attuned system very close to boundary conditions. Small resonantly amplified forces regularly applied to such systems could account for the observed variation. Until further research can establish the magnitude of forces required to sustain cybernetic feedback, a causal explanation for the correlations observed can be no more than tentative. The author wishes to stimulate the interest of those with better access to data and better analytic capability so progress can be made on this subject. The goal is accurate shorter and longer term prediction of changing solar activity. This ability will become more policy relevant as natural cyclic variations are increasingly recognised as important climate variables.

Table A1. Rotation ratios of secondary and non-adjacent planet pairs. Figures in bold indicate members of the Fibonacci series.

Other pairs	Rotation period	Rotations	Elapsed time	Ratio/sum	% match	For general interest only
1 Venus	243.02 days	1	243.02 d	243 + 1 =	99.99	(N3) 244 × (5/2) = 610
2 Earth	1 day (N3)	243	1 d	244 (N4)		(N4) Ve compared to 365.25 = 3 : 2 (99.8 %)
1 Mars	24.6229 hours	67	1649.7343 h	67 + 166 =	99.87	
2 Jupiter	9.925 hours	166	1647.55 h	**233**		
1 Saturn	640 min (N5)	3	1920 min	3 + 2 =	Up to 100	(N5) Re. Saturn: 644.4 min = 100 % match
2 Uranus	966.6 min	2	1933.2 min	**5**	(N1)	
1 Neptune	17.24 hours	80	1379.2 h	80 + 9 =	99.97	
2 Pluto	153.29 hours	9	1379.61 h	**89**		
Non-neighbours	Rotation period	Rotations	Elapsed time	Ratio/sum	% match	For general interest only
1 Jupiter	9.925 hours	13	129.025 h	13 + 8 =	99.888	
2 Uranus	16.11 hours	8	128.88 h	**21** (N6)		(N6) 13/8 = 1.625
1 Saturn	10.666 hours (N7)	21	223.986 h	21 + 13 =	Up to 100	(N7) 10.666 h = 640 min
2 Neptune	17.24 hours	13	224.12 h	**34** (N8)	(N1)	(N8) 21/13 = 1.6153846
1 Jupiter	9.925 hours	148	1468.9 h	148 + 85 =	99.76	
2 Neptune	17.24 hours	85	1465.4 h	**233**		
1 Uranus	16.11 hours	19	306.09 h	19 + 2 =	99.84	
2 Pluto	153.29 hours	2	306.58 h	**21**		
1 Neptune	17.24 hours	3	51.72 h	3 + 2 =	99.85	
2 Eris	25.9 hours (N2)	2	51.8 h	**5**		
1 Uranus	16.11 hours	8	128.88 h	8 + 5 =	99.52	
2 Eris	25.9 hours (N2)	5	129.5 h	**13**		
1 Jupiter	9.925 hours	63	625.275 h	63 + 26 =	99.8	63 = 21 × 3
2 Earth	24 hours	26	624 h	**89**		26 = 2 × 13
1 Mars	24.6229 hours	14	344.7206 h	14 + 20 =	99.977	
2 Neptune	17.24 hours	20	344.8 h	**34**		
1 Mars	24.6229 hours	57	1403.5053 h	57 + 87 =	99.86	
2 Uranus	16.11 hours	87	1401.57 h	**144**		
1 Mars	24.6229 hours	27	664.8183 h	27 +62 =	Up to 100	
2 Saturn	10.666 hours (N7)	62	661.33 h	**89**	(N1)	
1 Earth	24 hours	4	96 h	4 + 9 =	Up to 100	
2 Saturn	10.666 hours (N7)	9	96 h	**13**	(N1)	
1 Earth	24 hours	58	1392 h	58 + 86 =	99.53	
2 Uranus	16.11 hours	86	1385.46 h	**144**		

Table A2. In comparing real against randomly generated rotation ratios it is found that the real ratios obtain Fibonacci numbers around 50 % lower in value. This indicates that the real values are related in a non-random way. This makes the current theory that planetary rotation rates reflect the circumstances of the last collision the planetary bodies were involved in unlikely.

Real ratios		
Me Ve	99.797 %	116 + 28 = 144
Me Ve	99.851 %	795 + 192 = 987
Me Ve	99.986 %	1286 + 311 = 1597
Me Ve	99.992 %	8814 + 2132 = 10946
Me Ea	99.338 %	1570 + 27 = 1597
Me Ea	99.670 %	4111 + 70 = 4181
Me Ma	99.860 %	972 + 15 = 987
Me Ju	99.014 %	978 + 9 = 987
Me Ju	99.342 %	4143 + 38 = 4181
Me Ju	99.861 %	6704 + 61 = 6765
Me Sa	99.422 %	143 + 1 = 144
Me Sa	99.756 %	1586 + 11 = 1597
Me Ur	99.474 %	2554 + 30 = 2584
Me Ur	99.573 %	4132 + 49 = 4181
Me Ur	99.935 %	6686 + 79 = 6765
Me Ne	99.146 %	602 + 8 = 610
Me Ne	99.304 %	4127 + 54 = 4181
Me Ne	99.970 %	6677 + 88 = 6765
Ve Ea	99.214 %	2574 + 10 = 2584
Ve Ea	99.663 %	4165 + 16 = 4181
Ve Ea	99.905 %	6739 + 26 = 6765
Ve Ma	99.996 %	983 + 4 = 987
Ve Ju	99.996 %	6753 + 12 = 6765
Ve Ur	99.480 %	608 + 2 = 610
Ve Ne	99.558 %	6743 + 22 = 6765
Ea Ma	99.933 %	46 + 43 = 89
Ea Ma	99.988 %	510 + 477 = 987
Ea Ma	99.999 %	9151 + 8560 = 17 711
Ea Ju	99.421 %	70 + 19 = 89
Ea Ju	99.815 %	297 + 80 = 377
Ea Ju	99.848 %	777 + 210 = 987
Ea Ju	99.858 %	1258 + 339 = 1597
Ea Ju	99.971 %	2035 + 549 = 2584
Ea Ju	99.992 %	8620 + 2326 = 10 946
Ea Sa	99.902 %	64 + 25 = 89
Ea Sa	99.974 %	710 + 277 = 987
Ea Sa	99.995 %	4866 + 1899 = 6765
Ea Ur	99.219 %	88 + 56 = 144
Ea Ur	99.924 %	142 + 91 = 233
Ea Ur	99.997 %	973 + 624 = 1597
Ea Ur	99.999 %	6669 + 4277 = 10 946
Ea Ne	99.539 %	32 + 23 = 55
Ea Ne	99.838 %	84 + 60 = 144
Ea Ne	99.989 %	931 + 666 = 1597
Ea Ne	99.995 %	6381 + 4565 = 10 946
Ma Ju	99.809 %	101 + 43 = 144
Ma Ju	99.941 %	692 + 295 = 987
Ma Ju	99.982 %	2931 + 1250 = 4181
Ma Ju	99.986 %	4742 + 2023 = 6765
Ma Ju	99.998 %	7673 + 3273 = 10 946
Ma Sa	99.612 %	95 + 49 = 144

Table A2. Continued.

Real ratios		
Ma Sa	99.844 %	154 + 79 = 233
Ma Sa	99.948 %	249 + 128 = 377
Ma Sa	99.972 %	403 + 207 = 610
Ma Sa	99.997 %	652 + 335 = 987
Ma Ur	99.396 %	19 + 15 = 34
Ma Ur	99.743 %	211 + 166 = 377
Ma Ur	99.862 %	342 + 268 = 610
Ma Ur	99.987 %	553 + 434 = 987
Ma Ur	99.992 %	6133 + 4813 = 10 946
Ma Ur	99.994 %	9924 + 7787 = 17 711
Ma Ne	99.137 %	22 + 12 = 34
Ma Ne	99.676 %	93 + 51 = 144
Ma Ne	99.768 %	243 + 134 = 377
Ma Ne	99.871 %	637 + 350 = 987
Ma Ne	99.941 %	1030 + 567 = 1597
Ma Ne	99.987 %	1667 + 917 = 2584
Ma Ne	99.996 %	4364 + 2401 = 6765
Ju Sa	99.925 %	101 + 132 = 233
Ju Sa	99.992 %	692 + 905 = 1597
Ju Sa	99.994 %	4743 + 6203 = 10 946
Ju Sa	99.999 %	7674 + 10037 = 1771
Ju Ur	99.840 %	39 + 16 = 55
Ju Ur	99.967 %	1132 + 465 = 1597
Ju Ur	99.983 %	4795 + 1970 = 6765
Ju Ur	99.996 %	7758 + 3188 = 10 946
Ju Ne	99.969 %	75 + 69 = 144
Ju Ne	99.994 %	514 + 473 = 987
Ju Ne	99.995 %	3523 + 3242 = 6765
Ju Ne	99.998 %	9223 + 8488 = 17 711
Sa Ur	99.120 %	103 + 41 = 144
Sa Ur	99.835 %	167 + 66 = 233
Sa Ur	99.876 %	708 + 279 = 987
Sa Ur	99.949 %	1145 + 452 = 1597
Sa Ur	99.984 %	1853 + 731 = 2584
Sa Ur	99.990 %	2998 + 1183 = 4181
Sa Ur	100.000 %	4851 + 1914 = 6765
Sa Ne	99.040 %	2 + 1 = 3
Sa Ne	99.277 %	59 + 30 = 89
Sa Ne	99.688 %	155 + 78 = 233
Sa Ne	99.955 %	656 + 331 = 987
Sa Ne	99.970 %	1717 + 867 = 2584
Sa Ne	99.997 %	7274 + 3672 = 10 946
Ur Ne	99.095 %	27 + 28 = 55
Ur Ne	99.519 %	44 + 45 = 89
Ur Ne	99.949 %	71 + 73 = 144
Ur Ne	99.999 %	2062 + 2119 = 4181
Randomly generated rotation ratios		
Me Ve	99.962 %	116 + 28 = 144
Me Ve	99.984 %	795 + 192 = 987
Me Ve	99.998 %	8817 + 2129 = 10 946
Me Ea	99.409 %	1567 + 30 = 1597
Me Ea	99.630 %	2535 + 49 = 2584
Me Ea	99.995 %	4102 + 79 = 4181
Me Ma	99.718 %	1569 + 28 = 1597
Me Ma	99.858 %	4108 + 73 = 4181
Me Ju	99.133 %	1588 + 9 = 1597

Table A2. Continued.

Randomly generated rotation ratios		
Me Sa	99.844 %	2559 + 25 = 2584
Me Ur	99.728 %	1577 + 20 = 1597
Me Ur	99.939 %	6680 + 85 = 6765
Me Ne	99.828 %	230 + 3 = 233
Me Ne	99.858 %	4127 + 54 = 4181
Ve Ea	99.800 %	1590 + 7 = 1597
Ve Ma	99.361 %	6732 + 33 = 6765
Ve Ju	99.296 %	6753 + 12 = 6765
Ve Sa	99.457 %	2579 + 5 = 2584
Ve Ur	99.074 %	6745 + 20 = 6765
Ve Ne	99.184 %	1592 + 5 = 1597
Ea Ma	99.593 %	46 + 43 = 89
Ea Ma	99.748 %	195 + 182 = 377
Ea Ma	99.936 %	316 + 294 = 610
Ea Ma	99.943 %	511 + 476 = 987
Ea Ma	99.989 %	827 + 770 = 1597
Ea Ma	99.999 %	9172 + 8539 = 17 711
Ea Ju	99.601 %	101 + 43 = 144
Ea Ju	99.862 %	264 + 113 = 377
Ea Ju	99.936 %	1119 + 478 = 1597
Ea Ju	99.957 %	1810 + 774 = 2584
Ea Ju	99.998 %	2929 + 1252 = 4181
Ea Sa	99.989 %	65 + 24 = 89
Ea Sa	99.999 %	7994 + 2952 = 10 946
Ea Ur	99.732 %	32 + 23 = 55
Ea Ur	99.957 %	575 + 412 = 987
Ea Ur	99.984 %	1505 + 1079 = 2584
Ea Ur	99.989 %	6376 + 4570 = 10 946
Ea Ne	99.657 %	132 + 101 = 233
Ea Ne	99.889 %	214 + 163 = 377
Ea Ne	99.937 %	346 + 264 = 610
Ea Ne	99.996 %	560 + 427 = 987
Ma Ju	99.352 %	114 + 30 = 144
Ma Ju	99.459 %	184 + 49 = 233
Ma Ju	99.910 %	298 + 79 = 377
Ma Ju	99.979 %	2043 + 541 = 2584
Ma Ju	99.994 %	8654 + 2292 = 10 946
Ma Sa	99.623 %	64 + 25 = 89
Ma Sa	99.756 %	271 + 106 = 377
Ma Sa	99.848 %	438 + 172 = 610
Ma Sa	99.999 %	709 + 278 = 987
Ma Ur	99.114 %	93 + 51 = 144
Ma Ur	99.985 %	150 + 83 = 233
Ma Ur	99.993 %	7047 + 3899 = 10 946
Ma Ne	99.800 %	129 + 104 = 233
Ma Ne	99.985 %	546 + 441 = 987
Ma Ne	99.995 %	3742 + 3023 = 6765
Ma Ne	99.998 %	9797 + 7914 = 17 711
Ju Sa	99.860 %	58 + 31 = 89
Ju Sa	99.931 %	1041 + 556 = 1597
Ju Sa	99.962 %	1685 + 899 = 2584
Ju Sa	99.997 %	2726 + 1455 = 4181
Ju Ur	99.251 %	62 + 27 = 89
Ju Ur	99.354 %	163 + 70 = 233
Ju Ur	99.714 %	263 + 114 = 377
Ju Ur	99.932 %	426 + 184 = 610

Table A2. Continued.

Randomly generated rotation ratios		
Ju Ur	99.933 %	689 + 298 = 987
Ju Ur	99.985 %	1115 + 482 = 1597
Ju Ur	99.986 %	7643 + 3303 = 10 946
Ju Ne	99.240 %	31 + 24 = 55
Ju Ne	99.587 %	132 + 101 = 233
Ju Ne	99.787 %	213 + 164 = 377
Ju Ne	99.974 %	345 + 265 = 610
Ju Ne	99.997 %	6190 + 4756 = 10 946
Sa Ur	99.613 %	5 + 3 = 8
Sa Ur	99.680 %	235 + 142 = 377
Sa Ur	99.788 %	381 + 229 = 610
Sa Ur	99.992 %	616 + 371 = 987
Sa Ur	100.000 %	4222 + 2543 = 6765
Sa Ne	99.931 %	3 + 2 = 5
Sa Ne	99.985 %	592 + 395 = 987
Sa Ne	99.995 %	1550 + 1034 = 2584
Ur Ne	99.802 %	104 + 129 = 233
Ur Ne	99.986 %	441 + 546 = 987
Ur Ne	99.993 %	3023 + 3742 = 6765
Ur Ne	99.995 %	4891 + 6055 = 10 946
Ur Ne	100.000 %	7914 + 9797 = 17 711

Acknowledgements. The author wishes to thank the following people for their generous assistance in the production of this unfunded work: Stuart Graham, Ian Wilson, Roy Martin, Wayne Jackson, Graham Stevens, Roger Andrews, and many other people offering insight and comment at “Tallbloke’s Talkshop”.

Edited by: N.-A. Mörner
Reviewed by: H. Jelbring and one anonymous referee

References

Abreu, J. A., Beer, J., Ferriz-Mas, A., McCracken, K. G., and Steinhilber, F.: Is there a planetary influence on solar activity?, Astron. Astrophys., A88, 1–9, 2012.

Akasofu, Syun-Ichi: On the Present Halting of Global Warming, Climate, 1, 4–11, 2013.

Barrow, J. D.: Chaotic Behaviour in General Relativity, Phys. Rep., 85, 1, 1982.

Callebaut, D. K., de Jager, C., and Duhau, S.: The influence of planetary attractions on the solar tachocline, J. Atmos. Sol.-Terr. Phy., 80, 73–78, 2012.

Callebaut, D. K., de Jager, C., and Duhau, S.: Reply to “The influence of planetary attractions on the solar tachocline” by N. Scafetta, O. Humlum, J. E. Solheim, K. Stordahl, J. Atmos. Sol.-Terr. Phy., 102, p. 372, 2013.

Cho, W. and Kim, J.: Enhanced core formation rate in a turbulent cloud by self-gravity, Mon. Not. R. Astron. Soc. Letters, 410, L8–L12, doi:10.1111/j.1745-3933.2010.00968.x, 2011.

Fairbridge, R. W. and Hillaire-Marcel, C.: An 8,000-yr palaeoclimatic record of the “Double-Hale” 45-yr solar cycle, Nature, 268, 413–416, 1977.

Hung, Ching-Cheh: Apparent Relations Between Solar Activity and Solar Tides Caused by the Planets, NASA/TM-2007-14817, 2007.

Johnson, J. A., Payne, M., Howard, A. W., Clubb, K. I., Ford, E. B., Bowler, B. P., Henry, G. W., Fischer, D. A., Marcy, G. W., Brewer, J. M., Schwab, C., Reffert, S., and Lowe, T. B.: Retired A Stars and Their Companions. VI. A Pair of Interacting Exoplanet Pairs Around the Subgiants 24 Sextanis and HD 200964 Astron. J., 141, 10 pp., 2011.

José, P. D.: Sun's motion and sunspots, Astron. J., 70, p. 193, 1965.

Koyré, A.: The Astronomical Revolution, Hermann Paris, Cornell University, 1973.

Levison, H. F., Morbidelli, A., Van Laerhoven, C., Gomes, R., and Tsiganis, K.: Origin of the Structure of the Kuiper Belt during a Dynamical Instability in the Orbits of Uranus and Neptune, Icarus, 196, 258–271, 2008.

Lykawka, P. S. and Mukai, T.: Dynamical classification of trans-neptunian objects: Probing their origin, evolution, and interrelation, Icarus, 189, 213–232, 2007.

McCracken, K. G., Beer, J., Steinhilber, F., and Abreu, J.: A phenomenological study of the cosmic ray variations over the past 9400 years, and their implications regarding solar activity and the solar dynamo, Sol. Phys., 286, 609–627, 2013.

Mitzenmacher, M.: A Brief History of Generative Models for Power Law and Log-normal Distributions, Internet Mathematics, 1, 226–251, 2004.

Mörner, N. A.: Solar Wind, Earth's Rotation and Changes in Terrestrial Climate, Physical Review & Research International, 3, 117–136, 2013.

Rebull, L. M., Johnson, C. H., Gibbs, J. C., Linahan, M., Sartore, D., Laher, R., Legassie, M., Armstrong, J. D., Allen, L. E., McGehee, P., Padgett, D. L., Aryal, S., Badura, K. S., Canakapalli, T. S., Carlson, S., Clark, M., Ezyk, N., Fagan, J., Killingstad, S., Koop, S., McCanna, T., Nishida, M. M., Nuthmann, T. R., O'Bryan, A., Pullinger, A., Rameswaram, A., Ravelomanantsoa, T., Sprow, H., and Tilley, C. M.: New Young Star Candidates in BRC 27 and BRC 34, Astron. J., 145, 15, doi:10.1088/0004-6256/145/1/15, 2013.

Scafetta, N.: Does the Sun work as a nuclear fusion amplifier of planetary tidal forcing? A proposal for a physical mechanism based on the mass-luminosity relation, J. Atmos. Sol. Terr. Phy., 81–82, 27–40, 2012a.

Scafetta, N.: Multi-scale harmonic model for solar and climate cyclical variation throughout the Holocene based on Jupiter-Saturn tidal frequencies plus the 11-year solar dynamo cycle, J. Atmos. Sol.-Terr. Phy., 80, 296–311, doi:10.1016/j.jastp.2012.02.016, 2012b.

Scafetta, N., Humlum, O., Solheim, J.-E., and Stordahl, K.: Comment on "The influence of planetary attractions on the solar tachocline" by Callebaut, de Jager and Duhau, J. Atmos. Sol.-Terr. Phy., 102, 368–371, 2013.

Solheim, J.-E.: The sunspot cycle length – modulated by planets?, Pattern Recogn. Phys., 1, 159–164, doi:10.5194/prp-1-159-2013, 2013.

Svalgaard, L. and Cliver, E. W.: A Floor in the Solar Wind Magnetic Field Astrophys. J., 661, L203–L206, 2007.

Wilson, I. R. G., Carter, B. D., and Waite, I. A.: Does a Spin-Orbit Coupling Between the Sun and the Jovian Planets Govern the Solar Cycle?, Publ. Astron. Soc. Aust., 25, 85–93, 2008.

Wolff, C. L. and Patrone, P.: A New Way that Planets Can Affect the Sun, Sol. Phys., 266, 227–246, 2010.